Authors' Response to Reviews of

South Asia anthropogenic ammonia emission inversion through assimilating IASI observations

Ji Xia*, Yi Zhou*, Li Fang, Yingfei Qi, Dehao Li, Hong Liao, and Jianbing Jin
Atmospheric Chemistry and Physics Discussions,

RC: Reviewers' Comment, AR: Authors' Response, □ Manuscript Text

General Comments:

RC: ***The authors have addressed most of my previous comments effectively, with a more logical structure and clearer figures. However, the following minor revisions are still required to strengthen the ms:***

Response to Referee #1: We would like to thank the referee for the careful review throughout the paper and the in-depth comments that help to improve our paper.

Specific Comments:

RC: ***1) Units consistency: NH_3 concentration units are inconsistently reported in the Introduction and Results sections. To improve readability, use uniform units throughout the manuscript. If necessary, provide both unit forms in the Introduction for clarity.***

AR: Thank you for your feedback. We have revised the units for NH_3 concentration in the Introduction to ensure consistency with the units used in the Results section. This modification should enhance the clarity and readability of the manuscript. The specific changes in the manuscript are as follows.

Text in manuscript

1 Introduction

….

Specifically, the annual average ammonia concentration across India is approximately 1.8–5.6 × 10^{16} mol cm^{-2}, while in the Indo-Gangetic Plain (IGP) of India, the concentration is double that of

other regions, reaching a peak of 11.5 × 10^{16} mol cm^{-2} during the high season in July (Kuttippurath et al., 2020).

RC: ***2) Both Metop-A and Metop-B data are used for 2019 but does not justify why both satellites are necessary instead of a single platform. Please clarify this choice in Section 2.1.***

AR: Thank you for your comment. The use of both Metop-A and Metop-B data for 2019 ensures data continuity and enhances the reliability of the observations. While a single satellite could provide sufficient data, using both platforms allows for redundancy, reducing the risk of data loss due to satellite malfunctions or other issues. Additionally, combining data from both satellites improves temporal and spatial coverage, resulting in more accurate and robust results. The specific changes in the manuscript are as follows.

Text in manuscript

2.1 IASI satellite measurements

…

Therefore, only the data from Metop-A and Metop-B within the 2019 time frame were used in this study. The use of both Metop-A and Metop-B data for 2019 ensures data continuity and enhances the reliability of the measurements. While a single satellite could provide sufficient data, using both platforms could improve temporal and spatial coverage, resulting in more accurate and robust results.

RC: ***3) To ensure robustness, include a brief intercomparison of NH3 concentrations derived from Metop-A and Metop-B. Alternatively, compare the IASI version 4 products with prior studies.***

AR: Thank you for your suggestion. To ensure robustness, we have included a brief intercomparison of NH_3 concentrations derived from both Metop-A and Metop-B satellites. As shown in the Fig. S1, despite some small differences, the data from both satellites exhibit consistent spatial patterns and concentration levels. Furthermore, the data from the two satellites can complement each other, which enhances the reliability of the results. The specific changes in the manuscript are as follows.

Text in manuscript

2.1 IASI satellite measurements

The use of both Metop-A and Metop-B data for 2019 ensures data continuity and enhances the

reliability of the measurements. While a single satellite could provide sufficient data, using both platforms could improve temporal and spatial coverage, resulting in more accurate and robust results. To ensure robustness, we have also made a brief comparison of the NH_3 column concentrations obtained from both Metop-A and Metop-B satellites, as shown in the Fig. S1. Despite some small differences, the data from both satellites are generally consistent in terms of spatial patterns and concentration levels. Additionally, the data from the two satellites can complement each other, indicating good reliability of the results across both platforms.

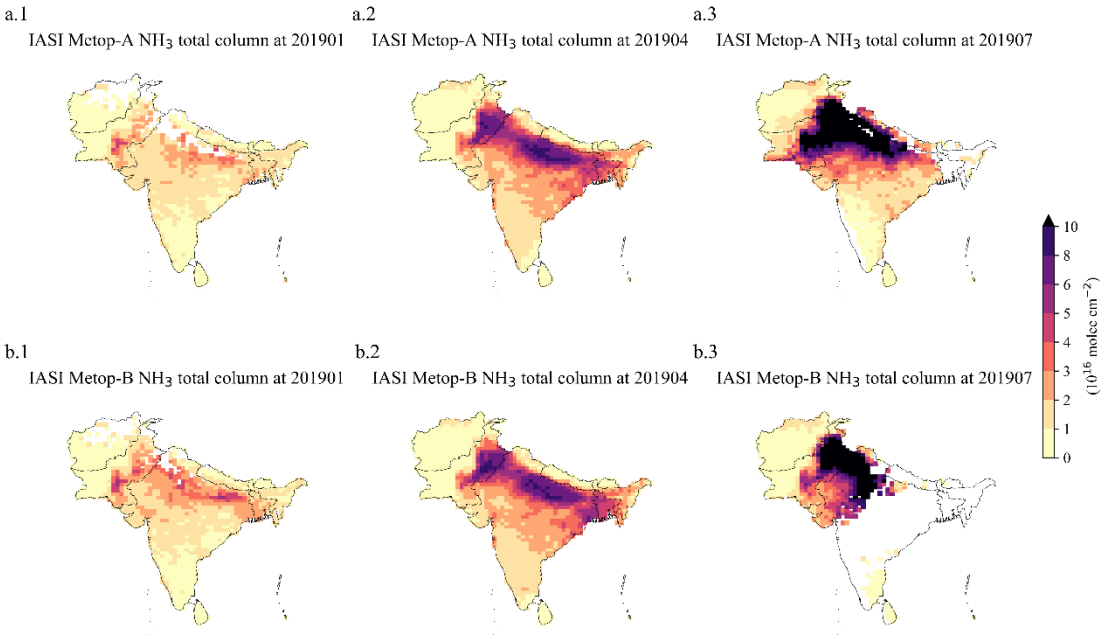

Figure S2. The distribution of IASI Metop-A (a) and Metop-B (b) NH_3 total column in 2019 January (a.1-b.1), April (a.2-b.2) and July (a.3-b.3).

RC: ***4) The exclusion of negative NH_3 total column values risks introducing a positive bias in gridded and monthly averages. Verify this by analyzing total columns in remote regions (e.g., oceans, deserts) where near-zero background concentrations are expected.***

AR: Thank you for your suggestion. We have re-compared the cases of excluding negative NH_3 total column values versus retaining them. As shown in the figure below, within our study region the effect on the final concentrations is minimal. However, we acknowledge that in remote regions (such as oceans and deserts) where near-zero background concentrations are expected, excluding negative values might introduce a positive bias. In future studies focusing on other regions, we will carefully re-evaluate and adjust our filtering criteria accordingly.

Text in manuscript

2.1 IASI satellite measurements

…

The assimilated observations for estimating the NH_3 emissions were the monthly IASI column concentration means over the 0.5 ◦× 0.625 ◦GEOS-Chem grid cell. These values were derived from the latest ANNI-NH_3-v4R-ERA5 product. Despite improvements in NH_3 column retrievals from satellite observations, there remains substantial variability in measurement uncertainty, ranging from 5% to over 1000% (Van Damme et al., 2014; Whitburn et al., 2016; Van Damme et al., 2017). Data selection was performed by excluding nighttime observations, irrational values (<0), and only using data with a cloud fraction < 0.1 (Van Damme et al., 2018) and skin temperature > 263 K (Van Damme et al., 2014) during the calculation of the monthly mean. While negative values are not necessarily incorrect, they are considered unrealistic in the context of NH3 concentrations. To improve the quality of the monthly average, we removed those negative values. Additionally, we have re-compared the cases of excluding negative NH_3 total column values versus retaining them. As shown in Fig. S2, the positive bias on the final concentrations within our study region is minimal.

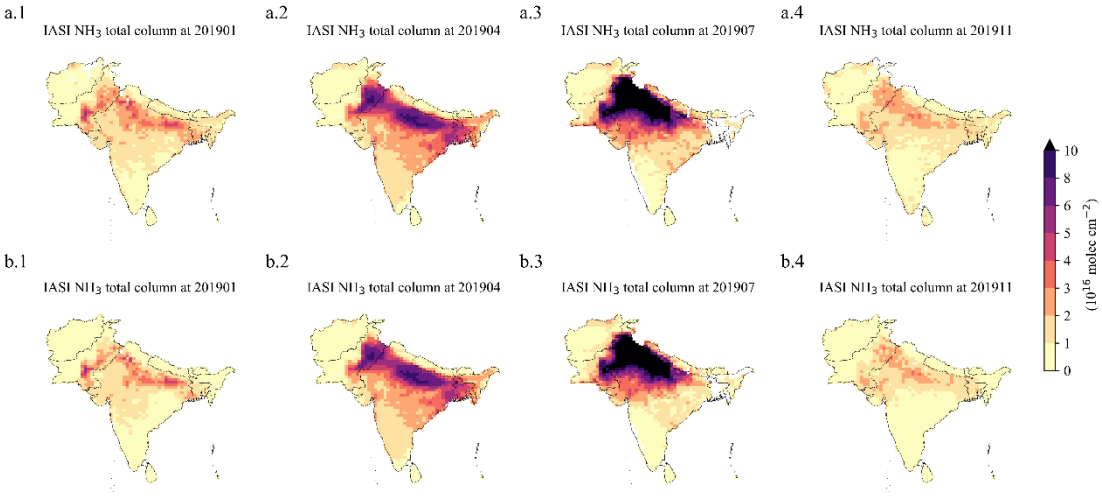

Figure S1. The distribution of IASI NH3 total column data in 2019. Panels (a.1)–(a.4) display the data after excluding negative values, while panels (b.1)–(b.4) display the data with negative values retained, corresponding to January, April, July, and November, respectively

RC: ***5) GEOS-Chem emission inventory: The revised manuscript implies that only anthropogenic emissions (CEDS) are used to drive GEOS-Chem, omitting natural/biomass burning sources. If true: 1. The title should reflect this limitation (e.g., "anthropogenic NH_3 emissions" instead of general "NH_3 emissions"). 2. Justify the exclusion of natural/biomass burning emissions in Section 2.4, especially given the seasonal mismatch between modeled (summer) and biomass burning (spring) peaks. 3. Clarify why a higher-resolution inventory (e.g., MIXv2) was not adopted, as coarse resolutions may misrepresent localized emission hotspots. If not: add related info into the Sect. 2.4.***

AR: Thank you for your feedback. We actually considered both natural and biomass burning sources to drive the GEOS-Chem model, but in this study, we primarily estimated the anthropogenic ammonia emissions inventory (CEDS). We have added natural and biomass burning sources information in Section 2.4 to clarify this point. Additionally, we have revised the explanation of the seasonal variation in emissions to avoid confusion between anthropogenic sources and biomass burning sources. We now focus solely on the seasonal variation of anthropogenic sources. The titile is now changed from "***South Asia ammonia emission inversion through assimilating IASI observations***" to "***South Asia anthropogenic ammonia emission inversion through assimilating IASI observations***"

We apologize for our previous inadequate response. Your recommendation is indeed useful. While high-resolution emission inversion is undoubtedly better, especially in capturing localized emission hotspots. Emission inversion for optimizing both the global and very local pattern also increases the computational load and requires more ensembles in our ensemble assimilation method. Otherwise, spurious correction introduced by the limited ensemble member will reduce the accuracy of the assimilation. Given our current limited computational resources, we chose not to adopt a higher-resolution inventory at this stage. However, we plan to consider using higher-resolution emission inventories, such as MIXv2, in future work to improve our results.

Text in manuscript

2.4 GEOS-Chem model and emission inventory

…

Specifically, these emissions stem predominantly from farmlands, including crops such as wheat, maize, and rice, as well as manure from livestock, including cattle, chicken, goats, and pigs (Liu et al., 2022). The CEDS emission estimates were coarse-grained into the model resolution 0.5◦× 0.625◦before being utilized to drive the GEOS-Chem simulations. Examples of the CEDS emission over the South Asia are presented in Fig. 3, which plot the total NH_3 emission fluxes for January, April, July, November of the year 2019. Additionally, the model's biogenic emissions are based on the MEGAN2.1 (Model of Emissions of Gases and Aerosols from Nature) inventory (Guenther et al., 2012), while the biomass burning sources driving the model are based on the GFEDv4 (Version 4 of the Global Fire Emissions Database) inventory (Giglio et al., 2013). The use of IASI and CrIS observations, along with GEOS-Chem simulations, is outlined in Table 1.

…

Country	Crop	Planting Period	Mid-Season	Harvest Period
Bhutan	Corn	Feb–Mar	Apr–Jun	Jul–Sep
India	Corn (Kharif)	Mar–Jun	Jul–Aug	Sep–Oct
India	Cotton	Apr–Jul	Aug–Sep	Oct–Dec
India	Millet (Kharif, Pearl)	May–Jul	Aug	Sep–Nov
India	Peanut (Kharif)	May–Jul	Aug	Sep–Nov
India	Rice (Kharif)	May–Jul	Aug	Sep–Nov
India	Sorghum (Kharif)	May–Jul	Aug	Sep–Oct
India	Soybean	Jun–Jul	Aug	Sep–Oct
India	Sunflowerseed (Kharif)	Jun–Jul	Aug	Sep–Oct
Nepal	Millet	May–Jul	Aug	Sep–Nov
Nepal	Rice	May–Jul	Aug–Sep	Oct–Dec
Pakistan	Corn	May–Jul	Aug	Sep–Oct
Pakistan	Cotton	Mar–Jun	Jul–Aug	Sep–Nov
Pakistan	Millet	May–Jun	Jul	Aug–Sep
Pakistan	Peanut	Mar–Jun	Jul	Aug–Oct
Pakistan	Rice	May–Jul	Aug	Sep–Nov
Pakistan	Sorghum	Jun–Jul	Aug	Sep–Oct
Pakistan	Sunflowerseed	Jan–Feb	Mar–May	Jun

Table 2. Crop calendars for selected Kharif crops in Bhutan, India, Nepal, and Pakistan from USDA.

3.2 NH3 emissions analysis

The substantial emissions in July, as indicated by the posterior inventory, can be attributed to the increased fertilizer application for crops during the summer season (Tanvir et al., 2019). As shown in Table 2, the sowing period for crops in South Asia is generally from May to July, with July being the peak growth period for crops, resulting in a large amount of fertilization, resulting in July surpassing May in emission intensity. From July to September, as rice and other crops progress through their growth stages, fertilizer application typically decreases, leading to a gradual reduction in NH_3 emissions. Additionally, temperatures decline from August to September Fig. S4 (b), reducing the volatilization rate of NH_3, thereby leading to a further decrease in emissions. This pattern occurs because NH_3 volatilization is strongly influenced by temperature (Fan et al., 2011).

RC: ***6) Table 1: 'Data' -> 'Data and model'***

AR: Thank you for your feedback. Thank you for your suggestion. We have updated Table 1 to change "Data" to "Data and model" as per your recommendation.

Table in manuscript

2.4 GEOS-Chem model and emission inventory

Data and Model	Period	Use
IASI v3	2015-2023	Annual variation of NH_3 concentration
IASI v4	entire 2019	Inversion and Validation
Level 2 CrIS	entire 2019	Independent validation
CPCB	entire 2019	Independent validation
GEOS-Chem	entire 2019	Similation

Table 1. The use of observations and simulations

RC: ***7) '3.2 Spatial and Seasonal variation of NH3 emission' -> 'NH3 emissions analysis'***

AR: Thank you for your suggestion. We have updated the section title from "3.2 Spatial and Seasonal variation of NH3 emission" to " Anthropogenic NH_3 emissions analysis" as recommended.

Text in manuscript

3.2 Anthropogenic NH_3 emissions analysis

RC: ***8) The ms cites USDA-derived planting/harvesting times to explain NH3 seasonality but does not present this data in the main text or supplement.***

AR: Thank you for your comment. We have now included the relevant information regarding USDA-derived planting/harvesting times to explain NH_3 seasonality. The specific changes made to the manuscript are as follows:

Text in manuscript

3.1.2 Seasonal and annual variation of NH3 concentration

We have identified the planting and harvesting times of crops in the South Asia region fr om USDA(U.S.DEPARTMENT OF ARGRICULTURE, https://ipad.fas.usda.gov/rssiws/al/crop _calendar/sasia.aspx), as presented in Table 2.

Country	Crop	Planting Period	Mid-Season	Harvest Period
Bhutan	Corn	Feb–Mar	Apr–Jun	Jul–Sep
India	Corn (Kharif)	Mar–Jun	Jul–Aug	Sep–Oct
India	Cotton	Apr–Jul	Aug–Sep	Oct–Dec
India	Millet (Kharif, Pearl)	May–Jul	Aug	Sep–Nov
India	Peanut (Kharif)	May–Jul	Aug	Sep–Nov
India	Rice (Kharif)	May–Jul	Aug	Sep–Nov
India	Sorghum (Kharif)	May–Jul	Aug	Sep–Oct
India	Soybean	Jun–Jul	Aug	Sep–Oct
India	Sunflowerseed (Kharif)	Jun–Jul	Aug	Sep–Oct
Nepal	Millet	May–Jul	Aug	Sep–Nov
Nepal	Rice	May–Jul	Aug–Sep	Oct–Dec
Pakistan	Corn	May–Jul	Aug	Sep–Oct
Pakistan	Cotton	Mar–Jun	Jul–Aug	Sep–Nov
Pakistan	Millet	May–Jun	Jul	Aug–Sep
Pakistan	Peanut	Mar–Jun	Jul	Aug–Oct
Pakistan	Rice	May–Jul	Aug	Sep–Nov
Pakistan	Sorghum	Jun–Jul	Aug	Sep–Oct
Pakistan	Sunflowerseed	Jan–Feb	Mar–May	Jun

Table 2. Crop calendars for selected Kharif crops in Bhutan, India, Nepal, and Pakistan from USDA.

RC: ***9) The text attributes lower July NH3 concentrations (vs. May) to higher temperatures enhancing volatilization, which may be a counterintuitive claim.***

AR: We agree that attributing the lower July NH_3 concentrations (compared to May) to higher temperatures enhancing volatilization is not entirely appropriate. We have revised the explanation to better reflect the combined impact of high temperatures and increased precipitation on NH_3 concentrations. The specific changes made to the manuscript are as follows:

Text in manuscript

3.1.2 Seasonal and annual variation of NH3 concentration

…

The reasons for higher emissions in July but lower concentration levels compared to May could be attributed to meteorological factors. The monsoon season in South Asia results in increased wet deposition, and notably, 2019 experienced the most intense monsoon since 1994 (NASA, 2020). As shown in the Fig. S4 (a) and (b), precipitation and temperature in July are the highest of the year. High temperature could increase ammonia volatilization, leading to higher concentrations, while high precipitation increases the wet deposition of ammonia. However, the impact of temperature on concentration is secondary compared to the dramatic variations in precipitation. These combined

factors result in July having a smaller concentration peak compared to May, despite July being another peak month.

RC: ***10) Add the number of your estimated budgets in the abstract and conclusion.***

AR: Thank you for your comment. I have already added the estimated budgets in both the abstract and conclusion sections of the document. The specific changes made to the manuscript are as follows:

Text in manuscript

Abstract. Ammonia has attracted significant attention due to its pivotal role in the ecosystem and its contribution to the formation of secondary aerosols. Developing an accurate ammonia emission inventory is crucial for simulating atmospheric ammonia levels and quantifying its impacts. However, current inventories are typically constructed in the bottom-up approach and are associated with substantial uncertainties. To address this issue, assimilating observations from satellite instruments for top-down emission inversion has emerged as an effective strategy for optimizing emission inventories. Despite the severity of ammonia pollution in South Asia, research in this context remains very limited. This study aims to estimate ammonia emissions in this region by integrating the prior emission inventory from the Community Emissions Data System (CEDS) and the columned ammonia concentration retrievals from the Infrared Atmospheric Sounder Interferometer (IASI). We employ a newly-developed four-dimensional ensemble variational (4DEnVar)-based emission inversion system to conduct the calculations, resulting in monthly ammonia emissions for 2019 at a resolution of 0.5◦×0.625◦. The annual total estimate for the posterior emission inventory is 12.61 Tg, compared to the prior inventory's 13.32 Tg. Our simulations, driven by the posterior emission inventory, demonstrate superior performance compared to those driven by the prior emission inventory. This is validated through comparisons against the IASI observations, the independent column concentration measurements from the advanced satellite instrument Crosstrack Infrared Sounder (CrIS), and the ground concentration observations of ammonia and PM2.5. Additionally, the spatial and temporal characteristics of ammonia emissions in South Asia based on the posterior are analyzed. Notably, emissions there exhibit a "double-peak" seasonal profile, with the maximum in July and the secondary peak in May. This differs from the "double-peak" trend suggested by the CEDS prior inventory, which identifies the maximum column concentration in May and a second peak in September. The differences may be attributed to a more accurate representation of regional agricultural practices, such as the timing of fertilizer application and meteorological influences like precipitation and temperature.

4 Summary and conclusion

…

The spatial and temporal characteristics of NH_3 emissions over South Asia were then analyzed based

on the inversion. While the prior CEDS inventory generally captured the NH_3 emission hotspots, such as in Pakistan, North India, and Bengal, it failed to accurately represent the seasonal trend. Specifically, the prior inventory showed a "double-peak" pattern throughout the year, with peaks in May and September. In contrast, the posterior results revealed the correct seasonal pattern with the "double-peak" profile occurring in May and July. The posterior emission inventory's total annual estimate is 12.61 Tg, compared to the prior inventory's 13.32 Tg.